mater.scichina.com link.springer.com

Published online 21 February 2023 | https://doi.org/10.1007/s40843-022-2351-y
Sci China Mater 2023, 66(6): 2283–2289

Fully conjugated two-dimensional sp^2-carbon covalent organic frameworks for efficient photocatalytic hydrogen generation

Hui Liu[1], Danbo Wang[1], Zefang Yu[1], Yajing Chen[2], Xubing Li[2], Ruiling Zhang[3], Xiong Chen[4], Lizhu Wu[2], Naixiu Ding[1*], Yuancheng Wang[1*] and Yingjie Zhao[1*]

ABSTRACT In this paper, two types of conjugated, triazine-based covalent organic frameworks (COFs) with different connected linkages (imine bond and sp^2-carbon–CN bond) are presented. The insignificant difference in the linkages creates a remarkable difference in their performance in visible-light-driven hydrogen generation. The fully π-conjugated two-dimensional (2D) COF with sp^2-carbon–CN linkages showed an external quantum efficiency of 13.48% at 450 nm, which is an unprecedented result for COF photocatalysts. In contrast, the imine-linked 2D COF displayed almost no photoactivity. Further photoelectrochemical and quantum chemical studies provide an in-depth understanding of the catalytic mechanism. This finding provides new insight into preparing high-performance organic photocatalysts for solar energy conversion.

Keywords: covalent organic frameworks, photocatalytic hydrogen generation, π-conjugated system, triazine

INTRODUCTION

Over the last few decades, photocatalytic hydrogen evolution (PHE) from water has become a promising method of producing clean and renewable energy sources. Continuous efforts have been devoted to developing new materials to achieve that purpose, among which photocatalysts are very effective [1–9]. PHE is a consecutive multistep process that requires systematic structural management and a suitable bandgap to restrict charge recombination and facilitate charge carrier generation and transport [10,11]. Hence, it is crucial to develop a highly efficient method for enhancing photocatalytic efficiency. Nonetheless, a simple principle for designing new and efficient photocatalysts is highly required. However, to date, the relationships between the atomic-level structures and the performance of photocatalysts remain unknown due to the lack of knowledge in the structures of photocatalysts [12–16].

Covalent organic frameworks (COFs) are crystalline organic porous polymers with well-defined structures and molecular tunability [17–20]. Moreover, COFs are believed to be potential photoactive materials for efficient solar energy conversion due to their long-range ordered structures, large surface areas, and tunable bandgaps [6,11]. Several COFs with photoactive functionalities, such as triazine [21,22], diacetylene [23], benzothiadiazole [24,25], thiazolo[5,4-*d*]thiazole [26], and sulfone [27] moieties have shown excellent photocatalytic activity. Another key factor that determines the performance of a photocatalyst is the linkages, which serve as a connection of the photoactive moieties. The reason for that is both electron transfer and light-absorbing behavior depend on the π-conjugation of the linkages. Imine [28–30], hydrazone [31,32], β-ketoenamine [33–35], triazine [22,36], and azine [37–39] have been widely used as typical linkages in the preparation of photoactive COFs for PHE.

Recently, sp^2-carbon-based COFs have been successfully constructed through Knoevenagel and aldol condensation [40,41]. Compared with the traditional imine-based COFs, the conjugation of the sp^2-carbon-based COFs is effectively enhanced. The fully conjugated sp^2-carbon linkages can improve the photothermal stability as well as broaden the visible light absorption range. Meanwhile, exciton migration and electron delocalization are greatly enhanced, resulting in promoted charge career mobility, which further facilitates the transfer of the photogenerated excitons to the surface of the photocatalyst. Moreover, sp^2-carbon-linked COFs are stable in the air under light illumination. Some remarkable studies [42–46] on the preparation of sp^2-carbon-linked COFs and their photocatalytic applications have already been reported. Although fully conjugated sp^2-carbon-linked COFs have many advantages, poor reversibility of this linkage makes the construction of sp^2-carbon-linked COFs very challenging. Additionally, the poor self-adjusting process does not promote the formation of highly ordered structures. Thus, many problems still exist regarding the preparation of these –C=C– linked COFs with good PHE activity and the atomistic structure-property relationships of COF materials in PHE.

Here, two triazine-based two-dimensional (2D) COFs (PTPA-COF with imine linkage and TP-COF with sp^2-carbon linkage) were prepared, and their PHE activities were compared. TP-COF exhibited a superior photocatalytic activity with an external quantum efficiency (EQE) of 13.48% among the COF photocatalysts, while PTPA-COF displayed almost no photoactivity.

[1] College of Polymer Science and Engineering, Qingdao University of Science and Technology, Qingdao 266042, China
[2] Key Laboratory of Photochemical Conversion and Optoelectronic Materials, Technical Institute of Physics and Chemistry, Chinese Academy of Sciences, Beijing 100190, China
[3] Institute of Molecular Sciences and Engineering, Institute of Frontier and Interdisciplinary Science, Shandong University, Qingdao 266237, China
[4] Key Laboratory of Molecule Synthesis and Function Discovery (Fujian Province University), State Key Laboratory of Photocatalysis on Energy and Environment, College of Chemistry, Fuzhou University, Fuzhou 350108, China
* Corresponding authors (emails: nxding1717@163.com (Ding N); wangyuancheng@qust.edu.cn (Wang Y); yz@qust.edu.cn (Zhao Y))

Furthermore, photocurrent, electrochemical impedance spectroscopy (EIS), femtosecond transient absorption (fs-TA) spectroscopy, and quantum chemical calculations were performed to explore the mechanism and the different performances between the two COFs. Moreover, the structure-activity relationship of the COFs with different linkages was investigated, which enables us to find a novel approach for improving the photocatalytic performance of COF materials.

EXPERIMENTAL SECTION

Chemicals and materials

Organic solvents 1,4-dioxane, tris(2-hydroxyethyl)amine (TEOA), *L*-ascorbic acid, and *n*-butyllithium (2.4 mol L^{-1} solution in hexanes) were purchased from Adamas. Cesium carbonate was procured from J&K Scientific. 1,4-Phenylenediacetonitrile was purchased from Sigma. Tetrahydrofuran (THF) was redistilled under argon reflux with Na crumbs. All aqueous solutions were prepared with Milli-Q water. All chemicals were used as received.

Synthesis of PTPA-COF

A 10-mL pyrex tube was charged with 2,4,6-tris(4-formylphenyl)-1,3,5-triazine (39.9 mg, 0.1 mmol), 2-phenylenediamine (16.3 mg, 0.15 mmol), THF (2 mL), dimethylacetamide (DMAC) (1 mL), and aqueous acetic acid (0.3 mL, 6 mol L^{-1}). This mixture was sonicated for 2 min, degassed through three freeze-pump-thaw cycles, sealed under vacuum, and heated at 120°C for 3 days. The reaction mixture was cooled to room temperature, and the precipitate was centrifuged and washed with H_2O and THF several times and dried under vacuum at 120°C for 10 h to afford an orange powder with a 87% isolated yield.

Synthesis of TP-COF

The synthesis of TP-COF was similar to that of PTPA-COF except that the pyrex tube was charged with 2,4,6-tris(4-formylphenyl)-1,3,5-triazine (25.2 mg, 0.064 mmol), 2-phenylacetonitrile (16.0 mg, 0.096 mmol), 1,4-dioxane (2 mL), and cesium carbonate (124 mg, 0.575 mmol). A yellow powder with a 82% isolated yield was obtained as TP-COF.

RESULTS AND DISCUSSION

PTPA-COF and TP-COF were prepared according to a previously reported method (Fig. 1a) [47,48]. The successful formation of the chemical bonds in PTPA-COF and TP-COF was confirmed by Fourier transform infrared (FT-IR) spectroscopy and ^{13}C cross-polarization magic angle spinning solid-state nuclear magnetic resonance (CP-MAS ssNMR) spectroscopy. Fig. S1a, b illustrate the FT-IR spectra of PTPA-COF, TP-COF,

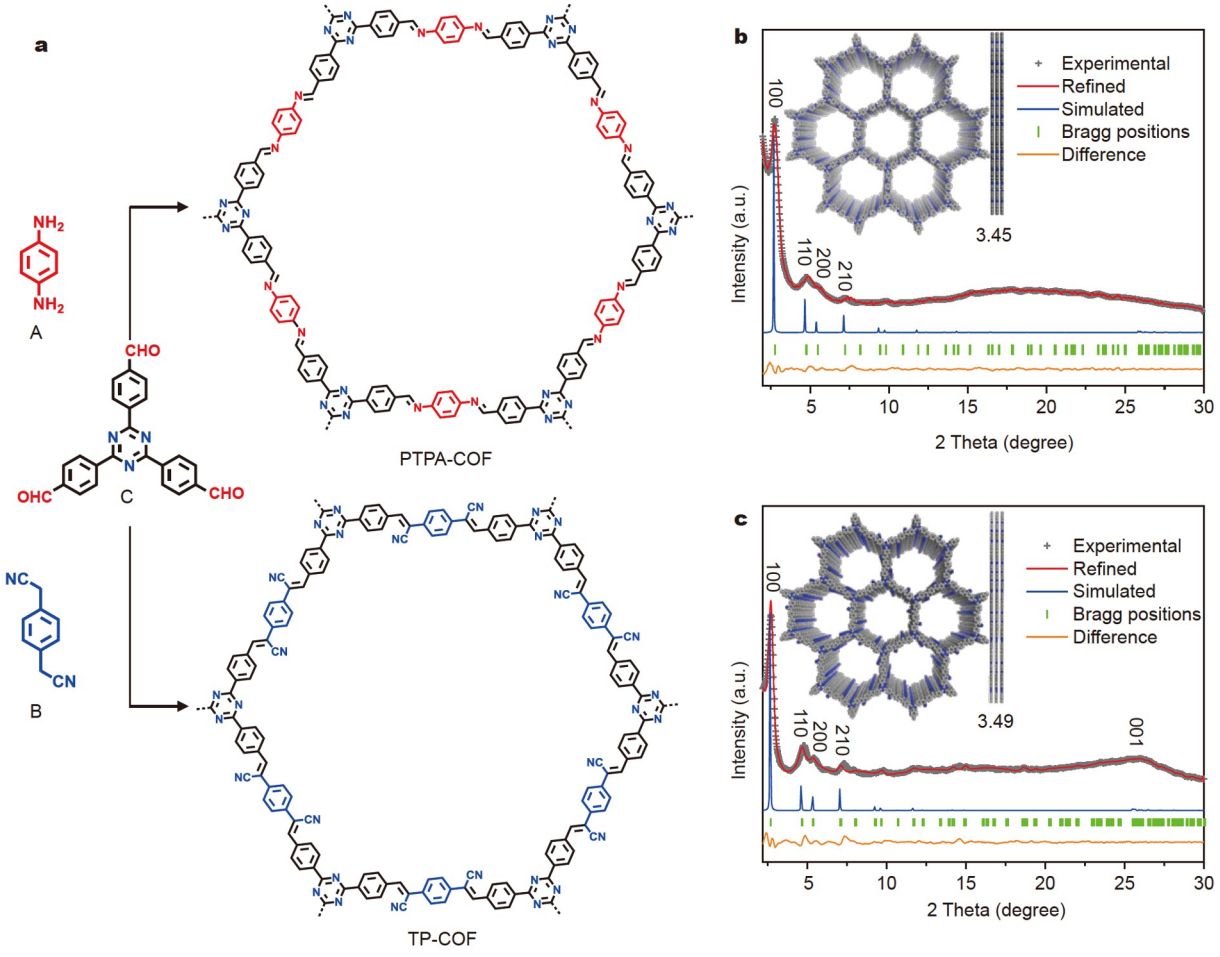

Figure 1 (a) Illustration of synthetic procedures of PTPA-COF and TP-COF by Schiff base condensation and Knoevenagel condensation, respectively. (b, c) PXRD patterns for PTPA-COF and TP-COF, and the insets are structural models of PTPA-COF and TP-COF assuming the AA stacking mode.

and monomers. The C=O stretching vibration of the aldehyde monomers at about 1700 cm^{-1} was significantly reduced, indicating the occurrence of polymerization. The stretching vibration peaks of the C=N bond at 1630 cm^{-1} in PTPA-COF and the C≡N bond at 2200 cm^{-1} in TP-COF further confirm the successful synthesis of the corresponding COF skeletons. Fig. S2 exhibits the ^{13}C NMR spectra of PTPA-COF and TP-COF. The corresponding peaks are well assigned. Hence, the chemical structures of the obtained COFs are well elucidated. The signal at ~158 ppm corresponding to imine carbon confirmed the formation of the imine linkage in PTPA-COF. Moreover, the signals at ~111 and ~118 ppm indicated the existence of the –C–CN linkage in TP-COF. Furthermore, the thermogravimetric analysis measurement verified the good thermal stability of PTPA-COF and TP-COF (Fig. S3). Notably, the decomposition temperature of TP-COF with C=C linkages is up to 500°C with less than 10% weight loss in N_2, indicating its better thermal stability than PTPA-COF. The two COFs exhibited rod-like morphology, as seen in their scanning electron microscopy (SEM) images (Fig. S4a, b). The high-resolution transmission electron microscopy (HR-TEM) images of TP-COF and PTPA-COF revealed the honeycomb-like internal structures (Fig. S4c, d).

Powder X-ray diffraction (PXRD) analyses revealed that the two COFs were crystalline. Combined with structural simulations, the experimental PXRD patterns of PTPA-COF and TP-COF were subjected to powder indexing. The diffraction peaks at 3.01°, 4.89°, 5.62°, 7.55°, and 24.8° were indexed to the (100), (110), (200), (210), and (001) reflections for PTPA-COF. Similarly, the PXRD pattern of TP-COF showed five distinguishable peaks at 2.78°, 4.78°, 5.45°, 7.34°, and 24.3°. Materials Studio software was used for the optimization of the geometric energy of structural models, and Pawley refinement was performed on the diffraction patterns. The experimental PXRD pattern was well-consistent for both of these COFs. Here, the simulated pattern was obtained from an AA stacking model. The refined parameters for the unit cells of PTPA-COF and TP-COF were $a = b = 37.502$ Å, $c = 3.449$ Å, $\alpha = \beta = 90°$, $\gamma = 120°$ (residuals $R_p = 4.58\%$, $R_{wp} = 6.21\%$) and $a = b = 37.514$ Å, $c = 3.488$ Å, $\alpha = \beta = 90°$, $\gamma = 120°$ (residuals $R_p = 3.51\%$, $R_{wp} = 4.47\%$), respectively.

N_2 adsorption-desorption was then conducted to evaluate the porous characteristics of the two COFs (Fig. S5). By employing the Brunauer-Emmett-Teller (BET) model, the surface areas of PTPA-COF and TP-COF were calculated to be 582 and 232 $m^2 g^{-1}$, respectively. A nonlocal density functional theory (NLDFT) cylindrical pore model was employed to elucidate the pore size distributions. Prominent distribution peaks at 2.41 and 2.32 nm were found for PTPA-COF and TP-COF, respectively. The experimental values are consistent with the theoretical values based on the Connolly surface in the AA stacking models.

Next, we studied the photophysical properties of PTPA-COF and TP-COF. PTPA-COF and TP-COF were orange and yellow in color, respectively, visible to the naked eye (Fig. S6). In Fig. 2a, PTPA-COF shows slightly red-shifted absorption (540 nm) compared with TP-COF (514 nm), as observed from the ultraviolet-visible (UV-vis) diffuse reflectance spectrum. The bandgaps of PTPA-COF and TP-COF were determined to be 2.31 and 2.43 eV, respectively, from the absorption spectra (Fig. 2b) [44]. The lowest unoccupied molecular orbital (LUMO) levels of PTPA-COF and TP-COF were estimated to be −3.35 and −3.23 eV by cyclic voltammetry measurements (Fig. S7) [42]. The highest occupied molecular orbital (HOMO) levels of both PTPA-COF and TP-COF were then calculated to be −5.66 eV (Fig. 2c). With the knowledge of the suitable bandgaps and the unique 2D conjugated structures of the obtained COFs, light-induced photocatalytic hydrogen evolution reaction (HER) of the two COFs was then executed.

The PHE of PTPA-COF and TP-COF was evaluated by taking a suspension of each COF material (5 mg) in water (25 mL) and irradiating it with visible light ($\lambda > 420$ nm) at 5°C. TEOA (10 vol%, pH 10.30) was chosen as the sacrificial electron donor (SED). H_2PtCl_6 (8 wt%) was added for the *in situ* formation of the Pt co-catalyst to facilitate hydrogen gas evolution from the surface of the materials. Consequently, the average HER yield of TP-COF reached as high as 29.12 mmol $h^{-1} g^{-1}$. In sharp contrast, PTPA-COF, structurally similar to TP-COF, presented a relatively low HER yield of 36 μmol $h^{-1} g^{-1}$ (Fig. 3a). Subsequently, the PHE performances of TP-COF and PTPA-COF with different SEDs were investigated. In Fig. S8, TP-COF exhibited the best performance for H_2 evolution when TEOA was used as the SED. Meanwhile, when 0.1 mol L^{-1} ascorbic acid solution was used as the SED, the HER rate of TP-COF decreased sharply to about 1/10 of the value in the presence of TEOA. Moreover, when a mixture of Na_2S/Na_2SO_3 aqueous solution was used as the SED, the PHE performance almost disappeared. For PTPA-COF, the HER yields were all poor in the presence of these three SEDs. The correlation between the HER yields of TP-COF and the Pt loading amount was then studied. The HER yields of 6, 12, 25, 37, and 50 μL H_2PtCl_6 (8 wt%)-modified TP-COF were 140.1, 169.5, 188.3, 122.8, and 117.8 μmol h^{-1}, respectively (Fig. S9), among which the HER yield corresponding to the 25 μL H_2PtCl_6-modified TP-COF is the best, which was thus selected to evaluate the stability. The reaction was run for 20 h in total and recorded every 5-h interval

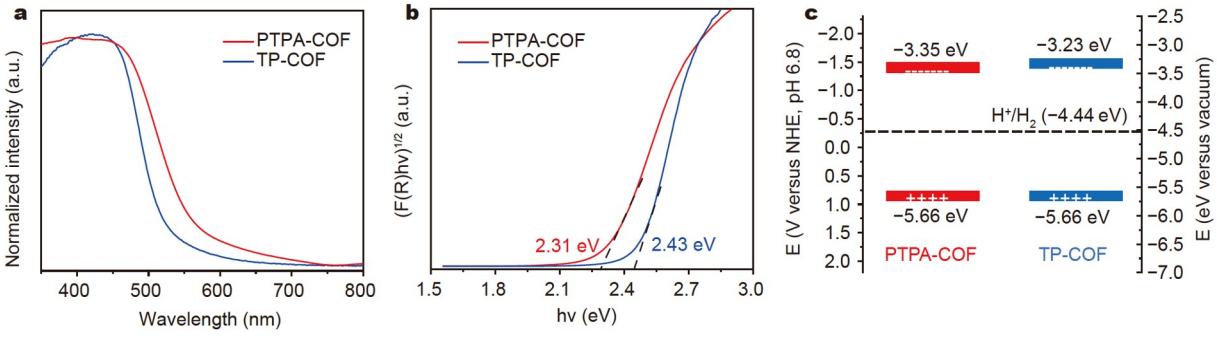

Figure 2 (a) Solid-state UV-vis spectra; (b) Tauc plots; and (c) band positions of PTPA-COF and TP-COF.

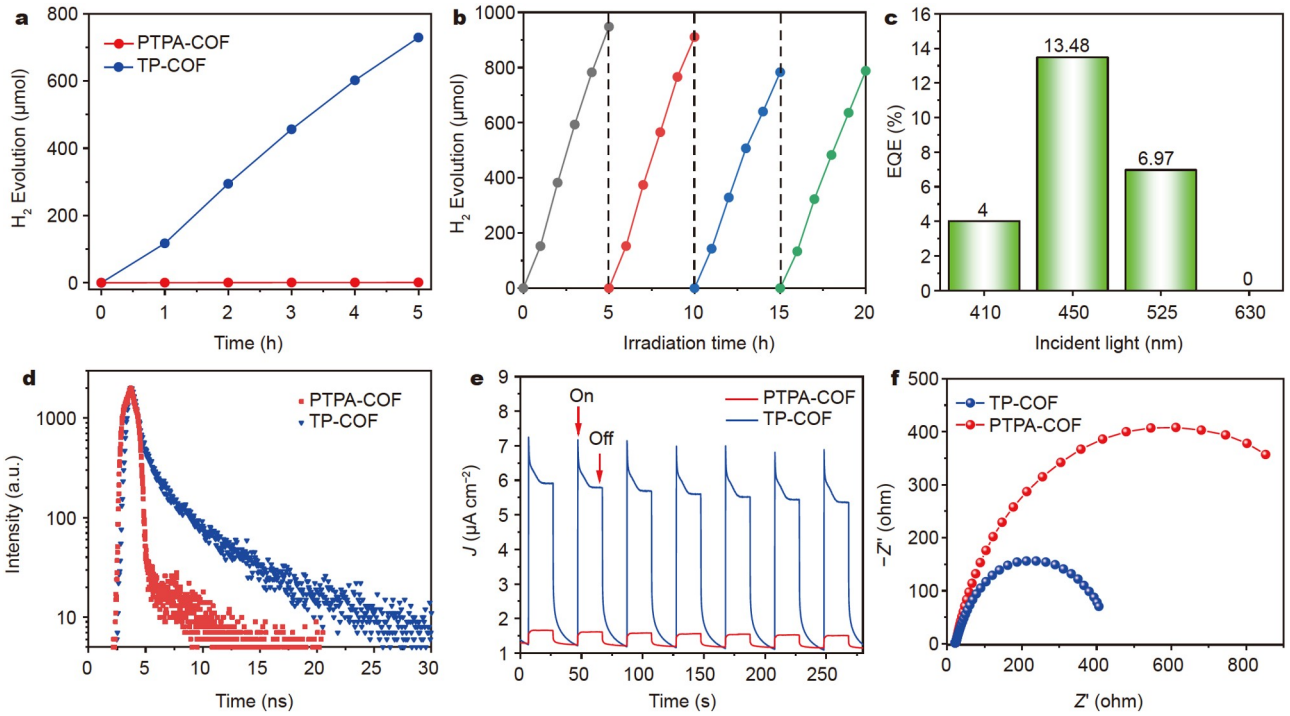

Figure 3 (a) Time-course hydrogen evolution using PTPA-COF and TP-COF as photocatalysts under visible-light (λ > 420 nm) irradiation. (b) Hydrogen production monitored over 20 h with TP-COF as the photocatalyst under visible-light (λ > 420 nm) irradiation (evacuation every 5 h). (c) EQEs of TP-COF under irradiation with monochromatic light at 410, 450, 525, and 630 nm. (d) Photoluminescence decay spectra of PTPA-COF and TP-COF. (e) Chopped photocurrent density *vs.* time recorded on PTPA-COF and TP-COF films. (f) EIS Nyquist plots of PTPA-COF and TP-COF film photoelectrodes.

under visible light irradiation (Fig. 3b). The total amount of H_2 evolved after 20 h was approximately 3620 μmol, which is far better than the previously reported HER yields of COF materials. These results also clarified that H_2O provided the prime source of hydrogen instead of COF itself. Moreover, FT-IR and PXRD analyses further demonstrated the good stability of TP-COF under prolonged light exposure (Fig. S10). The chemical composition and crystal structure of TP-COF showed no obvious change after the 20-h test. In addition, the SEM (Fig. S11a, b) and TEM (Fig. S11c) results of the recycled TP-COF after photocatalysis indicated no obvious changes, hence supporting the favorable stability of TP-COF in the HER process. Moreover, highly dispersed Pt nanoparticles were observed by TEM (Fig. S11d). Furthermore, we assessed the influence of the TP-COF dosage on photocatalytic activity. In Fig. S12, reducing the TP-COF dosage from 5 to 3 mg led to a slight reduction in HER yields from 29.12 to 28.53 mmol h^{-1} g^{-1}. However, increasing the TP-COF dosage from 5 to 10 mg significantly decreased the HER yields from 29.12 to 23.41 mmol h^{-1} g^{-1}. Moreover, the HER unexpectedly decreased from 23.41 to 14.86 mmol h^{-1} g^{-1} as the dosage of TP-COF increased from 10 to 20 mg. Under the same conditions, the presence of more catalysts lowers the HER yields, which may be caused by the aggregation of large amounts of TP-COF to form larger particles. Hence, this aggregation reduces the dispersion of TP-COF in the reaction solution, resulting in poor light absorption and transmittance and a low utilization rate of the active site of the photocatalyst. In addition, EQE is a key parameter for evaluating the ability of hydrogen generation by solar energy. This value is considered a standard for comparing the activities of different photocatalysts. In this study, the highest EQE obtained for TP-COF was 13.48% at 450 nm, which is an unprecedented value in organic COF materials (Table S1).

The excellent photocatalytic performance of TP-COF was achieved from its sp^2-carbon-linked fully π-conjugated structures. The more effortless the transfer of the photogenerated excitons is, the higher the charge carrier mobility is. PTPA-COF, in which the only structural difference from TP-COF is the linkage, is a perfect reference to verify this speculation. To further gain a deep understanding of the mechanism, first, the carrier generation and transport behavior of TP-COF was investigated upon irradiation. Photoluminescence decay curves were used to estimate the excited state lifetimes for the two COFs (Fig. 3d). The average weighted lifetime of TP-COF was measured to be 3.11 ns, which was remarkably longer than that of PTPA-COF (τ_{avg} = 0.25 ns). This result is consistent with the better photocatalytic ability of TP-COF. The much longer lifetime of TP-COF indicates the suppressed radiative recombination of photogenerated excitons due to its fully π-conjugated system. The transient photocurrent density of TP-COF is about 11 times as high as that of PTPA-COF (Fig. 3e), indicating that the fully π-conjugated system contributes to separating the photogenerated charges. The charge transfer process was further evaluated by the internal resistance through EIS measurement. In Fig. 3f, the EIS Nyquist plots manifest that TP-COF has a much smaller semicircle diameter than PTFT-COF, demonstrating the lower charge transfer resistance of TP-COF than that of PTFT-COF, which warrants efficient transportation and separation of charge carriers. Additionally, the frontier molecular orbitals and transmission functions of TP-COF and PTPA-COF were calculated to understand the effect of different linkages on the charge transport capability. In Fig. S13, two lin-

kages led to a clear difference in the transmission gap. The largest HOMO-LUMO gap is usually associated with charge carrier conductance. Generally, a narrower gap suggests a facilitated charge transport process [49]. The P_{11} (HOMO) and P_{12} (LUMO) peaks for the C=C linkage are located at −1.56 and 1.65 eV, respectively, indicating a gap of 3.21 eV. The P_{21} and P_{22} peaks at −1.59 and 1.89 eV, respectively, for the C=N linkage, correspond to a gap of 3.48 eV. The C=C linkage affords a narrower gap, indicating a more efficient charge transport process over the 2D conjugated molecular skeleton compared with the C=N COF (PTPA-COF).

To further clarify the role of the linkages in PHE activity and study the charge carrier dynamics, fs-TA was performed on the two COFs [50,51]. In Fig. 4a, upon excitation at 450 nm, TP-COF presents a strong positive signal in the 500–760 nm range, which can be attributed to a higher electron polaron yield and more efficient charge separation and accumulation of long-lived electrons. Meanwhile, for PTPA-COF, only a weak absorption on a shorter timescale of 2–8 ps was observed (Fig. 4b). The negligible absorption indicates a weak absorption cross-section for the trapped electrons. From the kinetic analysis of the two COFs (Fig. 4c, d), TP-COF displays a long-lived excited state absorption decay of 319.5 ps, which is much longer than that (18.1 ps) of PTPA-COF. These are achieved from the larger photogenerated electron population in TP-COF (electron polarons). In principle, the long lifetime of the excited state absorption is consistent with the highly efficient charge separation and transfer [52,53]. The different linkage structures in the COFs become a major contributory factor for the different photophysical properties. Moreover, the electron-withdrawing cyano group and triazines act as electron acceptors and benzene knots in the COF as the electron-donating moiety enable the formation of the A_1–D–A_2 system. The push-pull interactions and the fully π-conjugated linkages between D and A moieties successfully facilitate the transfer process of the photoexcited electrons from D to A moieties, thereby advancing the spatial electron-hole separation [54]. Finally, the hydrophilicity of the two COF structures was measured. The results revealed that the contact angle decreased from 123.1° for PTPA-COF to 91.3° for TP-COF (Fig. S14), indicating the better hydrophilicity of TP-COF. This may be due to the better hydrophilicity of sp^2-carbon–CN linkages. The high hydrophilicity facilitates the contact between the COF surface and the photocatalytic reaction solution, thus further enhancing the photocatalytic activity. Hence, TP-COF with cyano-based-sp^2 C=C linkages has better efficient charge separation and transfer kinetics and leads to higher PHE performance.

COF photocatalysis is a complicated and synergistic process determined by multiple electronic and structural factors. As demonstrated above, the correlation of crystallinity, porosity, and optical bandgaps between the two COFs was first explored. Similar crystallinity, stacking modes, and optical bandgaps were obtained for both COFs. However, compared with PTPA-COF, TP-COF featured a smaller BET value and weakened light energy collection but exhibited superior PHE activity to PTPA-COF. Thus, charge separation and transfer efficiency must be the core factors determining the PHE activity of COFs among the above-mentioned multiple elements [9]. The superior PHE activity of TP-COF should be derived from the excellent electron delocalization of the cyano-substituted sp^2 C=C linkages and the push-pull D–A interaction, which creates favorable molecular heterojunctions for highly efficient charge separation and

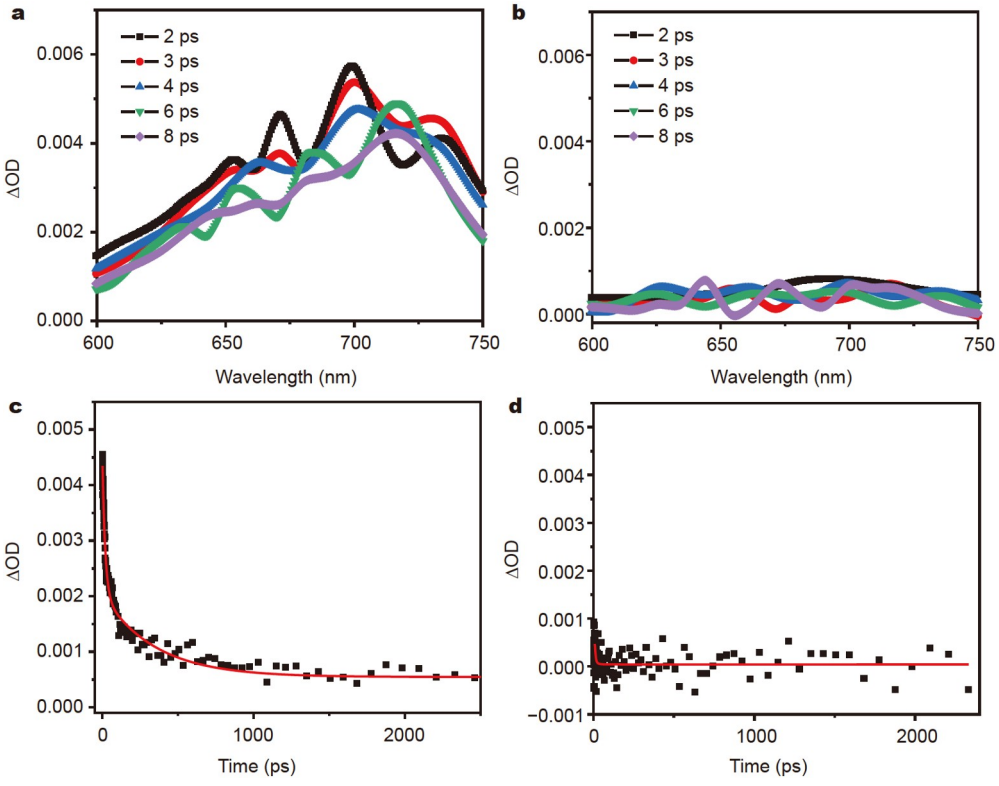

Figure 4 fs-TA spectra obtained from suspensions of (a) TP-COF and (b) PTPA-COF in 0.1 mg mL^{-1} aqueous solution containing 10 vol% TEOA. The corresponding kinetics of characteristic fs-TA absorption bands observed at 700 nm for the spectra of (c) TP-COF and (d) PTPA-COF.

transfer.

CONCLUSIONS

In conclusion, two COF materials linked by an imine bond (PTPA-COF) and an sp^2-carbon–CN bond (TP-COF), respectively, were synthesized. TP-COF yielded an EQE of 13.48% at 450 nm and a drastically higher HER yield of 29.12 mmol h^{-1} g^{-1} than its imine-linked counterpart (36 μmol h^{-1} g^{-1}). fs-TA spectroscopy and quantum chemical calculations revealed the key role of cyano-substituted sp^2 C=C linkages toward high-efficiency charge separation and transfer. The superior PHE performance of TP-COF was ascribed to the strong electron delocalization promoted by the fully conjugated linkages. This study provides a general guideline for the simple, effective and practical design of highly efficient COF-based photocatalytic materials.

Received 17 October 2022; accepted 5 December 2022; published online 21 February 2023

1 Fujishima A, Honda K. Electrochemical photolysis of water at a semiconductor electrode. Nature, 1972, 238: 37–38
2 Liu Y, Li B, Xiang Z. Pathways towards boosting solar-driven hydrogen evolution of conjugated polymers. Small, 2021, 17: 2007576
3 Naseri A, Samadi M, Pourjavadi A, *et al.* Graphitic carbon nitride (g-C_3N_4)-based photocatalysts for solar hydrogen generation: Recent advances and future development directions. J Mater Chem A, 2017, 5: 23406–23433
4 Nasir MS, Yang G, Ayub I, *et al.* Recent development in graphitic carbon nitride based photocatalysis for hydrogen generation. Appl Catal B-Environ, 2019, 257: 117855
5 Rodríguez-González V, Obregón S, Patrón-Soberano OA, *et al.* An approach to the photocatalytic mechanism in the TiO_2-nanomaterials microorganism interface for the control of infectious processes. Appl Catal B-Environ, 2020, 270: 118853
6 Wang H, Wang H, Wang Z, *et al.* Covalent organic framework photocatalysts: Structures and applications. Chem Soc Rev, 2020, 49: 4135–4165
7 Wang Y, Vogel A, Sachs M, *et al.* Current understanding and challenges of solar-driven hydrogen generation using polymeric photocatalysts. Nat Energy, 2019, 4: 746–760
8 Zhang W, Chen L, Dai S, *et al.* Reconstructed covalent organic frameworks. Nature, 2022, 604: 72–79
9 Zhang FM, Sheng JL, Yang ZD, *et al.* Rational design of MOF/COF hybrid materials for photocatalytic H_2 evolution in the presence of sacrificial electron donors. Angew Chem Int Ed, 2018, 57: 12106–12110
10 Chen X, Shen S, Guo L, *et al.* Semiconductor-based photocatalytic hydrogen generation. Chem Rev, 2010, 110: 6503–6570
11 Li Y, Song X, Zhang G, *et al.* 2D covalent organic frameworks toward efficient photocatalytic hydrogen evolution. ChemSusChem, 2022, 15: e202200901
12 Li G, Xie Z, Wang Q, *et al.* Asymmetric acceptor-donor-acceptor polymers with fast charge carrier transfer for solar hydrogen production. Chem Eur J, 2021, 27: 939–943
13 Chen J, Dong CL, Zhao D, *et al.* Molecular design of polymer heterojunctions for efficient solar-hydrogen conversion. Adv Mater, 2017, 29: 1606198
14 Lan ZA, Ren W, Chen X, *et al.* Conjugated donor-acceptor polymer photocatalysts with electron-output "tentacles" for efficient hydrogen evolution. Appl Catal B-Environ, 2019, 245: 596–603
15 Shu C, Han C, Yang X, *et al.* Boosting the photocatalytic hydrogen evolution activity for D-π-A conjugated microporous polymers by statistical copolymerization. Adv Mater, 2021, 33: 2008498
16 Wang L, Wan Y, Ding Y, *et al.* Conjugated microporous polymer nanosheets for overall water splitting using visible light. Adv Mater, 2017, 29: 1702428
17 Diercks CS, Yaghi OM. The atom, the molecule, and the covalent organic framework. Science, 2017, 355: eaal1585
18 Ding SY, Wang W. Covalent organic frameworks (COFs): From design to applications. Chem Soc Rev, 2013, 42: 548–568
19 Geng K, He T, Liu R, *et al.* Covalent organic frameworks: Design, synthesis, and functions. Chem Rev, 2020, 120: 8814–8933
20 Liu Y, Wu C, Sun Q, *et al.* Spirobifluorene-based three-dimensional covalent organic frameworks with rigid topological channels as efficient heterogeneous catalyst. CCS Chem, 2021, 3: 2418–2427
21 Ye H, Gong N, Cao Y, *et al.* Insights into the role of protonation in covalent triazine framework-based photocatalytic hydrogen evolution. Chem Mater, 2022, 34: 1481–1490
22 Zhang S, Cheng G, Guo L, *et al.* Strong-base-assisted synthesis of a crystalline covalent triazine framework with high hydrophilicity *via* benzylamine monomer for photocatalytic water splitting. Angew Chem Int Ed, 2020, 59: 6007–6014
23 Pachfule P, Acharjya A, Roeser J, *et al.* Diacetylene functionalized covalent organic framework (COF) for photocatalytic hydrogen generation. J Am Chem Soc, 2018, 140: 1423–1427
24 Chen W, Wang L, Mo D, *et al.* Modulating benzothiadiazole-based covalent organic frameworks *via* halogenation for enhanced photocatalytic water splitting. Angew Chem Int Ed, 2020, 59: 16902–16909
25 Zhao Z, Zheng Y, Wang C, *et al.* Fabrication of robust covalent organic frameworks for enhanced visible-light-driven H_2 evolution. ACS Catal, 2021, 11: 2098–2107
26 Li W, Huang X, Zeng T, *et al.* Thiazolo[5,4-*d*]thiazole-based donor-acceptor covalent organic framework for sunlight-driven hydrogen evolution. Angew Chem Int Ed, 2021, 60: 1869–1874
27 Wang X, Chen L, Chong SY, *et al.* Sulfone-containing covalent organic frameworks for photocatalytic hydrogen evolution from water. Nat Chem, 2018, 10: 1180–1189
28 Yang J, Acharjya A, Ye MY, *et al.* Protonated imine-linked covalent organic frameworks for photocatalytic hydrogen evolution. Angew Chem Int Ed, 2021, 60: 19797–19803
29 Sun L, Lu M, Yang Z, *et al.* Nickel glyoximate based metal-covalent organic frameworks for efficient photocatalytic hydrogen evolution. Angew Chem Int Ed, 2022, 61: e202204326
30 Li Y, Yang L, He H, *et al. In situ* photodeposition of platinum clusters on a covalent organic framework for photocatalytic hydrogen production. Nat Commun, 2022, 13: 1355
31 Stegbauer L, Schwinghammer K, Lotsch BV. A hydrazone-based covalent organic framework for photocatalytic hydrogen production. Chem Sci, 2014, 5: 2789–2793
32 Chen R, Wang Y, Ma Y, *et al.* Rational design of isostructural 2D porphyrin-based covalent organic frameworks for tunable photocatalytic hydrogen evolution. Nat Commun, 2021, 12: 1354
33 Ghosh S, Nakada A, Springer MA, *et al.* Identification of prime factors to maximize the photocatalytic hydrogen evolution of covalent organic frameworks. J Am Chem Soc, 2020, 142: 9752
34 Ming J, Liu A, Zhao J, *et al.* Hot π-electron tunneling of metal-insulator-COF nanostructures for efficient hydrogen production. Angew Chem Int Ed, 2019, 58: 18290–18294
35 Zhou T, Wang L, Huang X, *et al.* PEG-stabilized coaxial stacking of two-dimensional covalent organic frameworks for enhanced photocatalytic hydrogen evolution. Nat Commun, 2021, 12: 3934
36 Guo L, Niu Y, Xu H, *et al.* Engineering heteroatoms with atomic precision in donor-acceptor covalent triazine frameworks to boost photocatalytic hydrogen production. J Mater Chem A, 2018, 6: 19775–19781
37 Vyas VS, Haase F, Stegbauer L, *et al.* A tunable azine covalent organic framework platform for visible light-induced hydrogen generation. Nat Commun, 2015, 6: 8508
38 Banerjee T, Haase F, Savasci G, *et al.* Single-site photocatalytic H_2 evolution from covalent organic frameworks with molecular cobaloxime Co-catalysts. J Am Chem Soc, 2017, 139: 16228–16234
39 Stegbauer L, Zech S, Savasci G, *et al.* Tailor-made photoconductive pyrene-based covalent organic frameworks for visible-light driven hydrogen generation. Adv Energy Mater, 2018, 8: 1703278
40 Xu S, Richter M, Feng X. Vinylene-linked two-dimensional covalent organic frameworks: Synthesis and functions. Acc Mater Res, 2021, 2:

252–265
41 Pastoetter DL, Xu S, Borrelli M, *et al.* Synthesis of vinylene-linked two-dimensional conjugated polymers *via* the Horner-Wadsworth-Emmons reaction. Angew Chem Int Ed, 2020, 59: 23620–23625
42 Jin E, Lan Z, Jiang Q, *et al.* 2D sp^2 carbon-conjugated covalent organic frameworks for photocatalytic hydrogen production from water. Chem, 2019, 5: 1632–1647
43 Wei S, Zhang F, Zhang W, *et al.* Semiconducting 2D triazine-cored covalent organic frameworks with unsubstituted olefin linkages. J Am Chem Soc, 2019, 141: 14272–14279
44 Bi S, Yang C, Zhang W, *et al.* Two-dimensional semiconducting covalent organic frameworks *via* condensation at arylmethyl carbon atoms. Nat Commun, 2019, 10: 2467
45 Xu J, Yang C, Bi S, *et al.* Vinylene-linked covalent organic frameworks (COFs) with symmetry-tuned polarity and photocatalytic activity. Angew Chem Int Ed, 2020, 59: 23845–23853
46 Wang Y, Hao W, Liu H, *et al.* Facile construction of fully sp^2-carbon conjugated two-dimensional covalent organic frameworks containing benzobisthiazole units. Nat Commun, 2022, 13: 100
47 Qian HL, Li Y, Yan XP. A building block exchange strategy for the rational fabrication of *de novo* unreachable amino-functionalized imine-linked covalent organic frameworks. J Mater Chem A, 2018, 6: 17307–17311
48 Zhao Y, Liu H, Wu C, *et al.* Fully conjugated two-dimensional sp^2-carbon covalent organic frameworks as artificial photosystem I with high efficiency. Angew Chem Int Ed, 2019, 58: 5376–5381
49 Li X, Lei H, Liu J, *et al.* Carbon nanotubes with cobalt corroles for hydrogen and oxygen evolution in pH 0–14 solutions. Angew Chem Int Ed, 2018, 57: 15070–15075
50 Wang C, Mao X, Wang Z, *et al.* Synthesis and exciton dynamics of a one-dimensional organic copper halide perovskite. J Phys Chem C, 2022, 126: 4959–4964
51 Zhang R, Xu X, Mao X, *et al.* Excitation-dependent emission in all-inorganic lead-free $Cs_2ScCl_5{\cdot}H_2O$ perovskite crystals. Laser Photonics Rev, 2022, 16: 2100689
52 Kosco J, Sachs M, Godin R, *et al.* The effect of residual palladium catalyst contamination on the photocatalytic hydrogen evolution activity of conjugated polymers. Adv Energy Mater, 2018, 8: 1802181
53 Xiao JD, Shang Q, Xiong Y, *et al.* Boosting photocatalytic hydrogen production of a metal-organic framework decorated with platinum nanoparticles: The platinum location matters. Angew Chem Int Ed, 2016, 55: 9389–9393
54 Huang W, He Q, Hu Y, *et al.* Molecular heterostructures of covalent triazine frameworks for enhanced photocatalytic hydrogen production. Angew Chem Int Ed, 2019, 58: 8676–8680

Acknowledgements This work was financially supported by the National Natural Science Foundation of China (31202117 and 51972185) and the Natural Science Foundation of Shandong Province (ZR2020ZD38).

Author contributions Liu H carried out the synthesis and photocatalysis experiment and wrote the paper; Wang D did the quantum-chemical calculations; Yu Z helped with some synthesis work; Chen Y, Li X, and Wu L contributed to the photocatalytic performance tests and general discussion of photocatalysis; Zhang R performed the fs-TA spectra of the catalyst; Chen X helped analyze the mechanism; Ding N guided the quantum-chemical calculations; Wang Y guided the synthesis; Zhao Y guided the whole research and wrote the paper.

Conflict of interest The authors declare that they have no conflict of interest.

Supplementary information Experimental details and supporting data are available in the online version of the paper.

Hui Liu received his PhD degree from Qingdao University of Science and Technology in 2021. Now he is a post-doctoral researcher at Qingdao University of Science and Technology. His primary research interests focus on the preparation of highly conjugated COFs and photocatalytic applications.

Naixiu Ding obtained her PhD degree from Beihang University in 2011 and has been working at Qingdao University of Science and Technology since then. She is now a full professor at Qingdao University of Science and Technology. Her research interests focus on the structure and properties of polymer materials.

Yuancheng Wang received his PhD degree in 2018 from the Institute of Chemistry, Chinese Academy of Sciences, under the supervision of Prof. Deqing Zhang. Then, he joined Qingdao University of Science and Technology as a postdoctoral researcher and worked on the construction and applications of novel COFs under the supervision of Prof. Zhibo Li and Prof. Yingjie Zhao. In 2021, he joined the College of Polymer Science and Engineering, Qingdao University of Science and Technology. His current research focuses on the development of highly conjugated COFs and their potential applications in photocatalysis.

Yingjie Zhao obtained his PhD degree from the Institute of Chemistry, Chinese Academy of Sciences, in 2011. From 2011 to 2016, he did post-doctoral research at the University of Geneva and ETH Zürich. In 2016, he went back to China and joined Qingdao University of Science and Technology. Currently, he is a full professor at Qingdao University of Science and Technology. The research interests of Zhao's group focus on the design and synthesis of crystalline, highly conjugated 2D and 3D polymers and their photocatalysis applications.

二维sp^2碳共价有机框架及高效光催化制氢

刘辉[1], 王丹博[1], 于泽芳[1], 陈雅静[2], 李旭兵[2], 张瑞玲[3], 陈雄[4], 吴骊珠[2], 丁乃秀[1*], 王元成[1*], 赵英杰[1*]

摘要 本文设计合成了两种具有不同连接方式(亚胺键和sp^2-C–CN键)的三嗪基共价有机框架(COFs)材料. 连接单元的微小变化导致可见光驱动制氢性能的巨大差异. 具有sp^2碳连接方式的全π共轭二维COFs在450 nm波长处表现出13.48%的外量子效率, 优于已报道的COFs光催化剂. 而亚胺键的二维COFs几乎没有光活性. 借助光电化学研究和量子化学计算进一步研究了二维COFs的催化机理, 为太阳能转化高性能有机光催化剂的制备提供了新的见解.

